

Dynamics of Late-Stage Phase Separation: A Test of Theory

J. Alkemper,¹ V. A. Snyder,¹ N. Akaiwa,² and P. W. Voorhees^{1,*}

¹*Department for Materials Science and Engineering, Northwestern University, Evanston, Illinois 60208-3108*

²*Computational Materials Division, National Research Institute for Metals, 1-2-1 Sengen, Tsukuba, 305-0047, Japan*

(Received 13 November 1998)

The kinetics of Ostwald ripening are examined in a solid-liquid system that satisfies all assumptions of theory. We find that even at the longest coarsening time the samples are close to, but never reach, the steady-state coarsening regime. The coarsening rate agrees with predictions of the theories for transient Ostwald ripening to within the errors of the thermophysical parameters. These theories also describe the evolution of the particle size distribution very well. We thus conclude that the nonzero volume fraction theories of coarsening are sound. [S0031-9007(99)08766-9]

PACS numbers: 64.75.+g, 64.60.-i

Ostwald ripening, or coarsening, is a process in which the total particle-matrix interfacial area of a two-phase mixture decreases with time. It occurs via small particles dissolving and transporting their mass to large particles. It is an ubiquitous natural phenomena occurring in the late stages of virtually all phase separation processes.

The classical description of this process was given by Lifshitz and Slyozov [1] and Wagner [2] (LSW). They found that in the limit of a vanishing particle volume fraction and in the limit $t \rightarrow \infty$, where t is time, the system approaches a steady-state or self-similar regime in which the particle size distribution (PSD), when scaled by the average particle size, is time invariant and is independent of both the initial PSD and the materials parameters of the system. They also found that the average particle radius, \bar{R} , is given by the following temporal power law:

$$\bar{R}^3(t) = \bar{R}^3(0) + K_{\text{LSW}}t, \quad (1)$$

where K_{LSW} is the LSW rate constant. $K_{\text{LSW}} = 8T_0\Gamma D/9M_L(C_S - C_L)$ with T_0 the coarsening temperature, Γ the capillary length, D the diffusion coefficient, M_L the slope of the liquidus curve, and C_L and C_S the compositions of the solid and liquid at a planar solid-liquid interface.

More recently several theories have been developed that remove the restrictive assumption employed by LSW of a vanishingly small volume fraction of a coarsening phase [3–13]. It was found that in the limit $t \rightarrow \infty$ the exponents of the temporal power laws are unaltered, but the rate constant and shape of the scaled PSD become a function of the volume fraction. Specifically, the rate constant is predicted to vary with the volume fraction Φ as

$$K(\Phi) = K_{\text{LSW}}f(\Phi), \quad (2)$$

where $f(\Phi)$ is system independent. The scaled PSD's are predicted to be broader and more symmetric than those given by LSW.

It is fairly well established experimentally that the exponent of the temporal power for the average particle radius is indeed that predicted by theory. However, many of the other predictions of the theory remain unconfirmed. For example, beginning with the experiments of Ardell

[14,15] and continuing today [16], no measured PSD agrees with those given by theory. Also in contradiction to these theories are numerous reports that the rate constant is independent of the volume fraction [16,17]. However, this widely reported disagreement between theory and experiment (see, e.g., [17]) may be due to system dependent complications not included in the theory, such as elastic stress or fluid flow [18]. Thus, despite all the experiments that have been performed since the publication of the LSW papers, to the best of our knowledge none have employed systems that satisfy all the assumptions employed by theory and in which the thermophysical parameters needed to determine K_{LSW} have been measured independent of a coarsening experiment. We report here on experiments that are performed in such a system and thus allow us to address unambiguously the validity of a theory.

Previous work has identified solid-liquid mixtures consisting of solid Sn-rich particles in a Pb-Sn liquid as an ideal system to study coarsening phenomena: the particles are spherical, the coarsening rate is rapid, and the thermophysical parameters have been measured [19]. To access the low volume fractions at which most theories make predictions and to prevent both sedimentation of the particles and convection of the liquid matrix, these experiments were performed in microgravity during the space shuttle missions STS-83 and STS-94. A number of volume fractions ranging from 0.05 of Sn-rich particles up to 0.8 have been used for the experiments. The results presented here are for systems with a 10% coarsening phase, at which most theories make predictions. Other volume fraction samples have not yet been analyzed fully.

The samples were prepared in a similar manner to that done previously [20]. Samples were heated to a temperature of 185 °C, coarsened for times ranging from 70 s to more than 10 h, then quenched and stored. Isothermal conditions were achieved after 545 s of coarsening, and thus data for times less than this are not reported. Upon return to the laboratory, the samples were sectioned, etched, and photographed. Standard image analysis was performed on montages that were sufficiently large to encompass an entire cross section of a sample. Since all

the data were collected on plane sections, it is necessary to convert the theoretical predictions for \bar{R} and the particle size distribution to the corresponding quantities measured on a plane section, \bar{R}_{PS} and PSD_{PS} [21]. The kinetic equation for R_{PS} follows from Eqs. (1) and (2):

$$\bar{R}_{PS}^3(t) = \bar{R}_{PS}^3(0) + K_{PS}t, \quad (3)$$

with

$$K_{PS} = K_{LSW}f_{PS}(\Phi). \quad (4)$$

Each particle size distribution was determined by measuring ca. 4000 particles, thus allowing us to detect very small differences in PSD's measured at different times.

Grain boundary groove experiments allow K_{LSW} to be determined as a single quantity independent of a coarsening experiment. Hardy *et al.* measured $K_{LSW} = 1.01 \pm 0.05 \mu\text{m}^3/\text{s}$ (K_{LSW}^H) [19]. Similar experiments have been performed in microgravity along with the coarsening experiments. They yielded $K_{LSW} = 2.6 \pm 1.3 \mu\text{m}^3/\text{s}$ with the large scatter due to the limited number of data points. The higher value obtained in the spaceflight experiment indicates that there was no significant convection of the liquid in Hardy's experiments. One improvement was made to the grain boundary groove experiments, however, that could affect the results. In contrast to Hardy's experiments, we did not use flux in the preparation of the samples. This resulted in purer alloys and thus may have yielded a higher solid-liquid interfacial energy and the concomitantly higher K_{LSW} .

Typical microstructures of the solid-liquid mixtures are shown in Fig. 1. Clearly evident is the spherical morphology of the particles. The magnification of Figs. 1(a) and 1(b) are scaled by \bar{R}_{PS} such that the average particle radius shown in both figures is the same. The solid volume fraction obtained in all samples was 0.08–0.09.

Apparent in Fig. 1 is that the spatial distribution of the particles changed during coarsening. Analysis of the residual acceleration data during the MSL-1 missions shows that this change is not due to buoyancy driven particle movement [22]. To quantify the change in the spatial arrangement, the radial distribution (RDF) function on the plane sections was measured. It was found that

for early times the RDF undergoes significant changes while for the three longest coarsening times the RDF's seem to superimpose when the distance is scaled with the average particle size. A similar behavior was found for the PSD's. The scaled PSD's for three different times are shown in Fig. 2 together with a steady-state distribution and simulation results that will be discussed later. By comparing the PSD's to the steady-state distribution it is evident that the distributions are evolving with time. However, the distributions for the three longest experiments, only one of which is shown in Fig. 2, are very close to each other. It is not clear from these results if the system has reached steady state at the three longest times or if the evolution of the PSD and RDF are simply sufficiently slow that they appear to superimpose when scaled by \bar{R}_{PS} .

Nevertheless, we proceed in the standard fashion by assuming the presence of steady-state coarsening. A rate constant for the average particle radius was determined by regressing the average particle radius data measured on a plane section as a function of time, yielding $K_{PS} = 2.48 \pm 0.06 \mu\text{m}^3/\text{s}$ with a correlation coefficient of 0.999. The comparison of theory and experiment now is done in a rather unusual way: Using the measured K_{PS} and the $f_{PS}(0.1)$ predicted by different theories in Eq. (4) one can calculate K_{LSW} for each theory. These K_{LSW} 's can then be compared to K_{LSW}^H to determine the veracity of the theories. One can draw the same conclusions using this procedure as by comparing the measured and predicted K_{PS} , but it has the advantage that it can be used when the system is not in steady state as well. For the Marquess and Ross (MR), Akaiwa-Voorhees (AV), and Marsh and Glicksman (MG) theories we obtain $K_{LSW}^{MR} = 2.5$, $K_{LSW}^{AV} = 2.33$, and $K_{LSW}^{MG} = 2.06 \mu\text{m}^3/\text{s}$. These are factors of 2–2.5 higher than K_{LSW}^H . Most other theoretical predictions lie between the MG and MR theories.

If the steady-state regime has not been reached most theories cannot be compared to the experiments, since many theories assume that steady-state coarsening is present. It is clear from our experiments that at early stages non-steady-state coarsening was present. To determine if the system has reached steady state at the longest coarsening times the evolution of the particle size distribution was determined using two different theories. Both theories account for the effect of the interparticle diffusional interactions that occur at nonzero volume fractions. The first employs an AV simulation in which the growth rate of each particle is determined through a solution to the diffusion equation. The particles are placed randomly in a computational box and the box is repeated periodically to fill space. This approach has the advantage of accounting for the effects of the spatial distribution of particles and is free of any assumptions needed to determine the statistically averaged properties of these coarsening ensembles. The initial random spatial distribution of particles, however, differs from that found experimentally

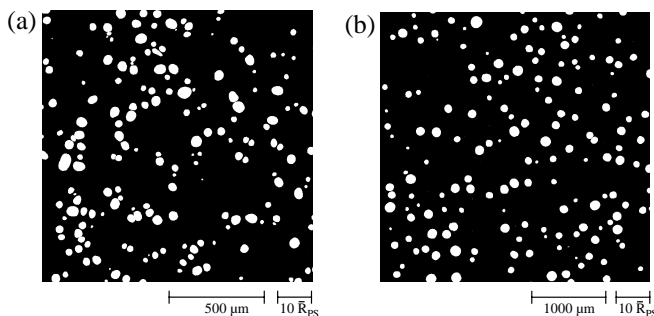


FIG. 1. Microstructures of the solid-liquid mixture after (a) 880 s of coarsening and (b) 36600 s of coarsening. The particles are white and the matrix is black.

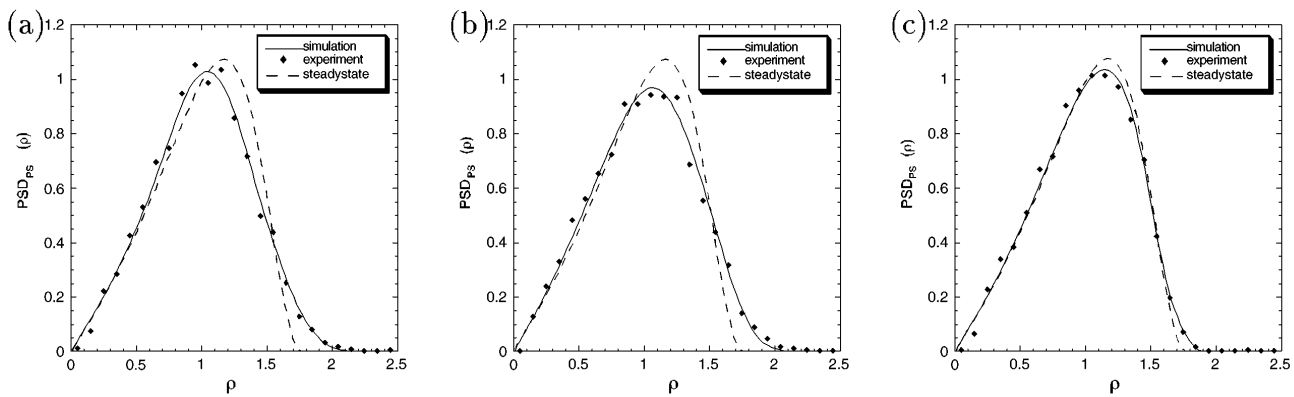


FIG. 2. Experimentally measured and calculated particle size distributions using the CV model at different times together with the steady-state prediction of the CV theory for (a) 880 s, (b) 2280 s, and (c) 36600 s of coarsening time. ρ is defined as $\rho = R_{PS}(t)/\bar{R}_{PS}(t)$.

at early times. Calculations that employ both the measured RDF's and PSD's as initial conditions are currently underway [23]. The disadvantage of this method is that only a limited number of particles can be used in the calculations; 10 000 particles were used at the beginning of coarsening. A second simulation was employed using a continuum model due to Chen and Voorhees (CV) [24] that incorporates the Marqusee-Ross expression [8] for the statistically averaged growth rate of a particle. This approach has the advantage that very long simulation times are possible, but rests upon a certain form for the statistically averaged growth rate of a particle. In both cases the experimentally measured PSD found after 545 s of coarsening was used as the initial PSD.

Figure 3 shows the theoretical predictions and the experimental results for the evolution of R_{PS} . Both theoretical predictions are nearly identical, thus, up to a constant, K_{LSW} , the temporal evolution of \bar{R} is independent of the model. In this case K_{LSW} is chosen for each simulation to yield the best possible fit to the experimental

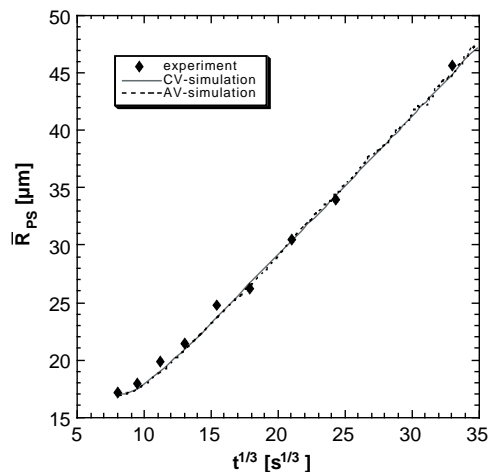


FIG. 3. The time dependence of the average particle size on a plane of section. The experimental values are shown together with the results from both simulations.

data. We obtain $K_{LSW}^{CV} = 2.0$ and $K_{LSW}^{AV*} = 1.9 \mu\text{m}^3/\text{s}$. These are lower than the values found assuming the presence of steady-state coarsening, specifically the disagreement between the K_{LSW} 's measured in the coarsening experiment and K_{LSW}^H has been reduced from a factor of 2.5 to 2 for the MR theory and from 2.3 to 1.9 for the AV theory. The remaining difference can be ascribed to impurity effects in the Hardy experiments, see above. These changes in K_{LSW} are large considering that the rate constants predicted by most theories agree to within 20% at $\Phi = 0.1$.

Figure 2 shows the evolution of the experimental and theoretical PSD. Since the AV model yielded very similar results to the CV model, only the latter is included. By comparing Figs. 2(a)–2(c) it is clear that the PSD first broadens [Figs. 2(a) and 2(b)] and then becomes sharper [Figs. 2(b) and 2(c)], with the maximum shifting to larger ρ . With further coarsening [Figs. 2(b) and 2(c)] the left side of the PSD remains nearly unchanged while the right side becomes steeper, the “tail” of the PSD's at large ρ becomes shorter, and the maximum becomes higher. The agreement between the experimentally measured and simulated PSD's is excellent. The simulations clearly show that the system is not in steady state. The PSD measured at the longest coarsening time is close to the predicted steady-state PSD, but differences are still evident. Other predictions of steady-state PSD's are in better agreement with the experimentally measured one shown in Fig. 2(c) than the CV-PSD, but still have a smaller largest particle size and higher maximum than the measured PSD. Calculations show that a considerably longer coarsening time is required for the PSD to become time independent, far longer than was accessible in these experiments.

In Fig. 4 a plot of the rate constant predicted by the CV theory as a function of time is shown. The AV theory predicts a very similar behavior to that of the CV theory. The plot shows quite clearly that the system is predicted to not be in steady state. The large change in

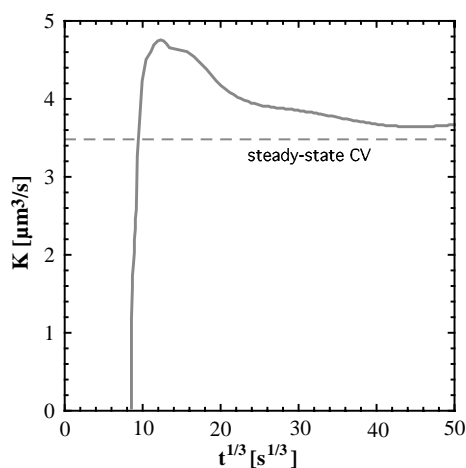


FIG. 4. The time dependence of the coarsening rate K for the CV simulation. Dimensional values for K and t were obtained using K_{LSW}^{CV} . The experimental data were obtained in the range $8 < t^{1/3} < 33 \text{ s}^{1/3}$.

the rate constant at early times predicted by the theories is unobservable experimentally due to the limited number of data points. Most of the data is acquired for $t^{1/3} > 12 \text{ s}^{1/3}$ where K is predicted to vary by only $\pm 10\%$ about the mean value and thus unobservable experimentally. The evolution of the rate constant reflects the approach of the system to the steady-state regime. It can be used as an indicator on how close the system is to steady state.

Both simulation and experiment show that the steady-state or self-similar regime has not been reached. It is the large number of particles used to determine the PSD along with the simulations that allows us to conclude that the system was not in steady state, as the differences in the PSD's and RDF's measured at the three longest coarsening times are very subtle. Usually it would have been assumed that steady-state conditions were present, especially since the regression showed that $\bar{R} \sim t^{1/3}$ to a high degree of confidence. However, due to the large number of particles used to characterize the state of the system, transient coarsening is clearly evident.

A quantitative comparison with theories other than CV and AV is not possible at this point. Once the kinetics and PSD's are measured for the other volume fractions employed in the spaceflight experiment, it may be possible to differentiate between the predictions of the many theories of Ostwald ripening. Samples with higher volume fractions of solid are in the process of being analyzed.

We have shown that there is an excellent agreement between the predictions of two theories for transient

Ostwald ripening and the measured coarsening rates and particle size distributions. The many past reports of disagreement between theory and experiment must thus be ascribed to phenomena that were present in the experiments and not accounted for in the theory or the undetected presence of transient coarsening.

We are grateful for very helpful discussions with A.J. Ardell. The financial support of the Microgravity Sciences Research Division of NASA is gratefully acknowledged.

*Author to whom correspondence should be addressed.

- [1] I.M. Lifshitz and V.V. Slyozov, *J. Phys. Chem. Solids* **19**, 35 (1961).
- [2] C. Wagner, *Z. Elektrochem.* **65**, 581 (1961).
- [3] M. Tokuyama, K. Kawasaki, and Y. Enomoto, *Physica (Amsterdam)* **134A**, 323 (1986).
- [4] Y. Enomoto, K. Kawasaki, and M. Tokuyama, *Acta Metall.* **35**, 907 (1987).
- [5] P.W. Voorhees and M.E. Glicksman, *Acta Metall.* **32**, 2001 (1984).
- [6] P.W. Voorhees and M.E. Glicksman, *Acta Metall.* **32**, 2013 (1984).
- [7] S.P. Marsh and M.E. Glicksman, in *Modelling of Coarsening and Grain Growth* (TMS, Warrendale, 1992).
- [8] J.A. Marqusee and J. Ross, *J. Chem. Phys.* **80**, 536 (1984).
- [9] M. Marder, *Phys. Rev. Lett.* **55**, 2953 (1985).
- [10] M. Marder, *Phys. Rev. A* **36**, 858 (1987).
- [11] A.D. Brailsford and P. Wynblatt, *Acta Metall.* **27**, 489 (1979).
- [12] C.W.J. Beenakker, *Phys. Rev. A* **33**, 4482 (1986).
- [13] N. Akaiwa and P.W. Voorhees, *Phys. Rev. E* **49**, 3860 (1994).
- [14] A.J. Ardell and R.B. Nicholson, *J. Phys. Chem. Solids* **27**, 1793 (1966).
- [15] P.K. Rastogi and A.J. Ardell, *Acta Metall.* **19**, 321 (1971).
- [16] W. Bender and L. Ratke, *Z. Metallkd.* **83**, 541 (1992).
- [17] A.J. Ardell, in *Proceedings of the Conference on Phase Transformations "87"* (The Institute of Metals, London, 1988), pp. 485–494.
- [18] P.W. Voorhees, *J. Stat. Phys.* **38**, 231 (1985).
- [19] S.C. Hardy, G.B. McFadden, S.R. Coriell, P.W. Voorhees, and R.F. Sekerka, *J. Cryst. Growth* **114**, 467 (1991).
- [20] S.C. Hardy and P.W. Voorhees, *Metall. Trans. A* **19**, 2713 (1988).
- [21] S.D. Wicksell, *Biometrika* **17**, 84 (1925).
- [22] J. Alkemper, V. Snyder, and P.W. Voorhees (to be published).
- [23] V. Snyder (unpublished).
- [24] M.K. Chen and P.W. Voorhees, *Model. Simul. Mater. Sci. Eng.* **1**, 591 (1993).